HHS Public Access

Author manuscript

Pediatr Neurol. Author manuscript; available in PMC 2016 June 01.

Published in final edited form as:

Pediatr Neurol. 2015 June ; 52(6): 615–623. doi:10.1016/j.pediatrneurol.2015.02.004.

Longitudinal Changes in Diffusion Properties in White Matter Pathways of Children with Tuberous Sclerosis Complex

Fiona M Baumer[a,†,*], **Jae W Song**[b,*], **Paul D Mitchell**[c], **Rudolph Pienaar**[d,e,f], **Mustafa Sahin**[a], **P Ellen Grant**[b,d,e,f], and **Emi Takahashi**[b,e,f,†]

[a]Department of Neurology, Boston Children's Hospital, Harvard Medical School, 300 Longwood Avenue, Boston, MA, 02115, USA

[b]Division of Newborn Medicine, Department of Medicine, Boston Children's Hospital, Harvard Medical School, 300 Longwood Avenue, Boston, MA, 02115, USA

[c]Clinical Research Center, Boston Children's Hospital, 300 Longwood Avenue, Boston, MA, 02115, USA

[d]Department of Radiology, Boston Children's Hospital, Harvard Medical School, 300 Longwood Avenue, Boston, MA, 02115, USA

[e]Athinoula A. Martinos Center for Biomedical Imaging, Massachusetts General Hospital, Harvard Medical School, 149 13th Street, Charlestown, MA, 02129, USA

[f]Fetal-Neonatal Neuroimaging and Developmental Science Center, Boston Children's Hospital, Harvard Medical School, 300 Longwood Avenue, Boston MA, 02115, USA

Abstract

Background—Abnormal white matter development in patients with Tuberous Sclerosis Complex (TSC), a multisystem hamartomatous disorder caused by aberrant neural proliferation and axonal maturation, may be associated with poorer neurocognitive outcomes. The purpose of this study is to identify predictors of longitudinal changes in diffusion properties of white matter tracts in patients with TSC.

Methods—Diffusion MRI was carried out in 17 subjects with TSC (mean age, 7.2 ± 4.4 years) with at least 2 MRIs (mean number of days between scans, 419.4 days ± 105.4 days). There were 10 males; 5 of 17 had autism spectrum disorder; and 10 of 17 had epilepsy. Regions of interest were placed to delineate the internal capsule/corona radiata, cingulum, and corpus callosum. The outcomes were mean change in apparent diffusion coefficient and fractional anisotropy. Data were analyzed using Pearson's correlation and multiple linear regression analyses.

[†]Correspondence should be addressed to: Emi Takahashi, Ph.D., Division of Newborn Medicine, Boston Children's Hospital, 1 Autumn St. #456, Boston, MA 02115, phone (617) 999-0433 | fax (617) 730-4671, emi.takahashioki@childrens.harvard.edu, emi@nmr.mgh.harvard.edu, Fiona Baumer, M.D., Department of Neurology, Boston Children's Hospital, Harvard Medical School, 300 Longwood, Avenue, Boston, MA, 02115, USA, Fiona.Baumer@childrens.harvard.edu.

[*]These authors equally contributed to this work.

Results—Gender was a significant predictor of mean change in apparent diffusion coefficient in the left internal capsule, right and left cingulum bundles, and corpus callosum and a significant predictor of mean change in fractional anisotropy in the corpus callosum. Epilepsy was a significant predictor of mean change in apparent diffusion coefficient in the left internal capsule. Autism spectrum disorder was not predictive of diffusion changes in any of the studied pathways.

Conclusion—Clinical variables, including gender and epilepsy, have an effect on the development of white matter pathways. These variables should be taken into consideration when counseling TSC patients and in future imaging studies in this population.

Keywords

Tuberous Sclerosis Complex; White Matter; Development; Human; Diffusion Imaging; Tractography; Epilepsy; Gender

INTRODUCTION

Tuberous sclerosis complex (TSC) is a multisystem hamartomatous disorder that affects 1 in 6,000 people. Most cases of TSC are linked to mutations in the *TSC1* and *TSC2* genes. The translated protein products from these genes help regulate cell growth and proliferation by inhibiting the mammalian target of the rapamycin (mTOR) cascade. In the developing brain, this aberrant proliferation leads to the formation of cortical tubers, subependymal nodules, and subependymal giant cell astrocytomas (SEGAs). Cells in the central nervous system express TSC1/2 proteins not only during early development but also throughout adulthood. These proteins are thought to help regulate functions such as axon guidance and myelination, dendritic arborization, and synaptic formation and function.[1,2]

Despite a growing understanding of the molecular changes occurring in TSC, correlating cellular changes with clinical phenotype remains challenging. This challenge is in part due to the wide spectrum of neurologic outcomes manifested by TSC patients. For example, 80–90% of the TSC patients develop epilepsy,[3,4] 50–60% show some degree of cognitive limitation,[3,5,6] and approximately 15–50% develop autism spectrum disorder (ASD).[6–8] However, to date, no consistent relationship between tuber location, burden or genotype with cognitive outcomes has been reported.[9,10]

Efforts have thus turned to diffusion tensor magnetic resonance imaging (DTI) to assess for any imaging correlates in subjects with TSC. DTI measures the diffusion of water molecules in the brain tissue. The magnitude of diffusion (apparent diffusion coefficient [ADC]) and the directionality of water movement (fractional anisotropy [FA]) provide information about tissue microstructure, including the degree of myelination and axonal membranes.[11] Interestingly, DTI studies show differences in diffusion properties not only in tubers[12,13] but also in normal appearing white matter in TSC patients when compared with control subjects.[14–17] Abnormal diffusion characteristics in normal appearing white matter (NAWM) in TSC subjects have been speculated to arise from diffuse abnormal neuronal and axonal organization and hypomyelination[18] though alternatively a recent study proposed that radial migration streams, which represent discrete but multifocal pathology, may cause the diffusion changes.[19]

Recent imaging studies have examined correlations between DTI parameters of NAWM and neurocognitive outcomes in TSC. Although region of interest (ROI) analysis looking at ADC and FA in NAWM in TSC subjects[12,20] has not demonstrated an association between diffusion properties with neurologic outcomes, tractography studies analyzing complete white matter tracts, such as the corpus callosum[18] and arcuate fasciculus[21] report significant differences not only in ADC and FA between TSC subjects and controls but also between TSC subjects with and without comorbid ASD. These findings suggest that abnormal white matter tract development in TSC patients may be associated with poorer neurocognitive outcomes. However, it remains unknown which white matter tracts are affected and how these affected tracts evolve over time.

To better understand the development of this disease process as it relates to white matter microstructural integrity, a subset of TSC patients who were serially scanned was identified and the change in ADC and FA of selected white matter tracts between scans (mean change) was measured. This outcome represents the magnitude of change of the diffusion parameter during the developmental period and provides insight about the neurologic evolution of the disease process. As prior studies suggest that neurocognitive outcomes are correlated with white matter microstructure, TSC subjects were categorized by neurocognitive outcomes, such as epilepsy and ASD. First, diffusion parameters were correlated with age to evaluate trends and changes in ADC and FA. Second, using multiple linear regression analyses, predictors of the magnitude of longitudinal change of the diffusion properties among the internal capsule/corona radiata, cingulum bundle and corpus callosum were identified using demographic characteristics and neurocognitive outcomes as variables. These tracts were selected as sample tracts from major commissural, projection and association pathways. These tracts have been associated with changes in diffusion or anisotropic properties in children with epilepsy[22–24] or autism spectrum disorder[18,25–27] and were thus selected for the study.

MATERIALS AND METHODS

Participants

The source population included patients who fulfilled the clinical criteria for tuberous sclerosis complex set forth by the Tuberous Sclerosis Consensus Conference[28,29] and participated in the Boston Children's Hospital Multi-disciplinary Tuberous Sclerosis Program. Eligible participants from this population were retrospectively identified by the following inclusion/exclusion criteria: greater than 1 year of age, 2 brain MRIs obtained at least 300 days apart, no neurosurgical interventions, were not enrolled in everolimus trials, no hydrocephalus on imaging, and adequate image quality without motion degradation. The Institutional Review Board at Boston Children's Hospital deemed this an exempt project because the research involved existing data with no risk to patient confidentiality.

Thirty-six subjects with 2 MRI scans were identified from the Tuberous Sclerosis Complex database. Nineteen subjects did not meet the eligibility criteria and were excluded, leaving seventeen subjects with TSC; (n = 9, excluded due to < 1 years old, prior neurosurgical intervention, or enrollment in therapeutic drug (everolimus) trial; n = 10, excluded due to poor quality of the MRI scans secondary to motion artifact). The mean age was 7.2 ± 4.4

years (range: 2.0 – 17.5 years), and 59% (n = 10) were male and 41% (n = 7) were female. The mean number of days that lapsed between the 2 MRI scans was 419 ± 105 (range: 309 – 741 days). Five subjects had autism spectrum disorder (ASD), and 10 subjects had epilepsy.

Imaging

High-angular resolution diffusion imaging (HARDI) is a technique that enables identification of complex crossing tissue coherence in mature[30] and immature brains with less myelin.[31–35] T1-weighted magnetization-prepared rapid-acquisition gradient-echo, T2-weighted turbo spin-echo, and a 3D diffusion-weighted spin-echo echo-planar imaging were performed. Thirty diffusion-weighted measurements (b = 1,000 sec/mm^2) and 5 non-diffusion-weighted measurements (b = 0 sec/mm^2) were acquired from a 3T Siemens MR system with TR (repetition time) = 10 sec; TE (echo time) = 88 msec; ∂ = 12.0 msec; Δ = 24.2 msec; field of view = 22 cm; slice thickness = 2.0 mm; matrix size = 128×128; iPAT = 2.

Diffusion Data Reconstruction for Tractography

Diffusion Toolkit and TrackVis (http://trackvis.org) were used to reconstruct and visualize HARDI tractography pathways. HARDI detects multiple local maxima on an orientation distribution function (ODF). Using all the ODF local maxima to produce HARDI tractography pathways permitted identification of crossing pathways within a voxel. Trajectories were propagated by consistently pursuing the orientation vector of least curvature. Tracking was terminated when the angle between 2 consecutive orientation vectors was greater than the given threshold (45°).[36]

Tract Delineation

A coordinate-based tractography atlas[37] was used to guide ROI placement to delineate white matter pathways on MRI datasets for each subject at the first scan (Scan 1) (Fig. 1). We used T1, T2 and diffusion images for placement of ROIs. ROIs were then co-registered using FLIRT software (http://fsl.fmrib.ox.ac.uk/fsl/fsl-4.1.9/flirt/overview.html) to each subject's second scan. Segmentation of each white matter tract pathway for the second scan was then checked manually to ensure accuracy and adjusted as needed. Mean ADC and mean FA for each tract was calculated. The corpus callosum, cingulum bundles, and bilateral internal capsule/corona radiata tracts were segmented.

Statistical Analysis

Descriptive data for continuous variables are presented as mean ± standard error (SE) and categorical variables as percentages and counts. Outcomes include the paired change in ADC and FA for each tract. Paired changes were calculated by subtracting the diffusion measurements at the time of the second scan (Scan 2) from those at the time of the first scan (Scan 1). Except for change in ADC for the corpus callosum, all outcomes were normally distributed per the Shapiro-Wilk test. Visual inspection of a Q-Q plot and a stem-and-leaf plot identified a single outlier in the distribution for change in ADC of the corpus callosum. Without this outlier, the remaining data were normally distributed, and a sensitivity analysis with and without this outlier showed consistent results.

Comparison of each outcome with each categorical variable was performed with the Student's *t* test. Correlations between continuous variables were assessed with Pearson's correlation coefficient (r). Due to the small sample size, nonparametric tests (Mann-Whitney *U* test and Spearman's correlation coefficient) were also performed to confirm the results. Only parametric results are shown because the results were consistent with the nonparametric tests.

Multiple linear regressions identified predictors of mean change in ADC or FA. Each model included the ADC or FA measure at scan 1 (baseline scan value) and one other predictor variable (age, gender, ASD, or epilepsy). Regression diagnostics, including residual plots and Q-Q plots, were used to evaluate assumptions of constant variance and normality. One influential outlier was identified; however, review of patient history and imaging was unremarkable from a clinical standpoint, and the subject was retained. Statistical significance was set at $P \leq 0.05$, and all tests were two-sided. All statistical analyses were performed with SPSS version 19.0 (IBM SPSS, Chicago, IL, USA).

RESULTS

Mean Changes in ADC and FA

Visual representations of absolute measures of FA and ADC in single subjects are shown in Figures 2–4. Figure 2 illustrates segmented white matter pathways from subjects with the lowest ADC (Fig. 2A) and highest ADC (Fig. 2B). Figure 3 illustrates male (Fig. 3A, C) and female (Fig. 3B, D) subjects, and Figure 4 illustrates subjects with (Fig. 4A, C) and without epilepsy (Fig. 4B, D).

Comparisons of the mean change in ADC and FA by gender, epilepsy, and ASD are shown in Table 1. A gender effect was seen in several of the white matter tract pathways. An increase in the mean change ADC was seen in males compared with a decrease in females in the left internal capsule (3.78 ± 6.17 mm^2/sec vs. -20.2 ± 7.92 mm^2/sec; $P = 0.03$) and left cingulum bundle (3.65 ± 3.21 mm^2/sec vs. -19.8 ± 5.98 mm^2/sec; $P = 0.002$). A significant difference in the mean change in FA between males and females in the corpus callosum was also seen (-0.02 ± 0.006 vs. 0.003 ± 0.009; $P = 0.04$).

Correlations Analyses

Table 2 reports correlations between age and ADC and FA. Age negatively correlated with ADC for both the right and left internal capsules at scan 1 [right: r = −0.62 ($P = 0.007$), left: r = −0.56 ($P = 0.02$)] and at scan 2 [right: r = −0.52 ($P = 0.03$), left: r = −0.59 ($P = 0.01$)]. Age positively correlated with FA for both the right and left internal capsules at scan 1 [right: r = 0.48 ($P = 0.05$), left: r = 0.52 ($P = 0.03$)] and at scan 2 [right: r = 0.47 ($P = 0.06$), left: r = 0.59 ($P = 0.01$)]. Age positively correlated with mean change ADC at scan 2 for the right internal capsule was also seen (r = 0.49, $P = 0.05$).

The left cingulum bundle demonstrated significant correlations between age and ADC [scan 1: r = −0.51 ($P = 0.04$), scan 2: r = −0.55 ($P = 0.02$)] and FA [scan 1: r = 0.53 ($P = 0.03$), r = 0.57 ($P = 0.02$)]. At scan 2, age positively correlated with FA in the right cingulum bundle (r = 0.51, P=0.04).

Neither ADC nor FA correlated with age in the corpus callosum. Age positively correlated with mean change in ADC at scan 2 (r = 0.55, $P = 0.02$).

Predictors of Mean Change in ADC Measures

For the left internal capsule, when controlling for the baseline scan ADC measure, the mean ADC change in males was 23.3 ± 8.29 mm^2/sec greater than in females ($P = 0.01$) and 22.5 ± 8.74 mm^2/sec greater in subjects with epilepsy than those without ($P = 0.02$) (Table 3). Relationships among gender, initial ADC scan measure, and mean ADC changes are illustrated in Figure 5.

The baseline ADC scan measure was a significant predictor of mean change in ADC for the right internal capsule when controlling for each subject characteristic ($P \leq 0.05$ for gender, epilepsy, and ASD). However, adjusting for baseline ADC scan measure, none of the subject characteristics emerged as significant predictors in the right internal capsule.

For the left and right cingulum bundles, only gender emerged as a significant predictor of the mean change in ADC (Table 3), controlling for the initial ADC scan measure. The mean change in ADC for males was 23.8 ± 6.4 mm^2/sec greater than for females in the left cingulum ($P = 0.002$) and 20.1 ± 9.0 mm^2/sec greater in the right cingulum ($P = 0.04$). Neither epilepsy, ASD nor the baseline ADC scan measure emerged as significant predictors in these models.

For the corpus callosum, because age and the baseline ADC scan measures were not significantly correlated (Table 2), an additional model including both independent variables was used to assess mean change in ADC. The baseline ADC scan measure was a significant predictor of the mean change in ADC after controlling for age (β = −0.24±0.11, $P = 0.05$), gender, (β = −0.32 ± 0.10, $P = 0.005$), epilepsy (β = −0.32 ± 0.12, $P = 0.02$), and ASD (β = −0.26 ± 0.13, $P = 0.05$). By contrast, when controlling for the baseline ADC scan measure, only gender emerged as a significant predictor; the mean change in males was 31.8 ± 14.6 mm^2/sec greater than in females ($P = 0.05$).

Predictors of Mean Change in Fractional Anisotropy Measures

For the left and right internal capsules and bilateral cingulum bundles, only the baseline FA scan measure emerged as a significant predictor of the mean change in FA when controlling for gender, epilepsy, and ASD in each respective model (Table 4). Controlling for the initial scan FA measure, gender emerged as a significant predictor of mean change in FA (β = 0.02 ± 0.007, $P = 0.003$) in the corpus callosum. Relationships among gender, baseline FA scan measure, and mean FA changes are illustrated in Figure 6.

DISCUSSION

This study is the first to describe evolving changes in the diffusion properties of developing white matter tracts in TSC subjects and the first to report tractography results for the complete internal capsule and cingulum in TSC subjects. Understanding the natural evolution of diffusion changes in patients with TSC is particularly timely and relevant as patients are currently undergoing therapeutic trials with mTOR-inhibitors that are

investigating these parameters. Tillema et al[38] analyzed serial MRIs in subjects with TSC and growing SEGAs. They reported that over the 12–18 month study period, subjects who received everolimus showed an increase in FA and a decrease in radial diffusivity in the corpus callosum, internal capsule and geniculo-calcarine regions compared with no change in diffusion parameters in subjects who did not undergo this treatment. The authors speculated that the improvement in white matter structural integrity was due to the drug effect but did not report on other clinical variables that could have an impact, such as the severity of epilepsy or presence of autism. Moving forward, it will be important to understand what other clinical factors have an impact on white matter organization before interpreting these treatment trials.

In this study, a significant gender effect in the mean change ADC, but not mean change FA, emerged in several white matter tracts. Our results also show that the mean change ADC in males is significantly smaller, by nearly 35 to 100 fold, than in females (Table 3). Interestingly, no gender effect was seen in the mean change in FA in any of the white matter tracts. In comparison, serial MRI studies of healthy subjects have not found a difference between genders in the magnitude of change of ADC or FA over time.[41–43] These results suggest that, on a microstructural level, the development of white matter pathways of the left internal capsule, bilateral cingulum bundles, and corpus callosum is delayed or decreased in males with TSC compared with females. Only a few studies have examined gender differences in TSC in the context of neurocognitive phenotypes. Studies report a significantly increased neurologic morbidity in males than females, as manifested by more cortical tubers and subependymal nodules and a higher incidence of epilepsy and intellectual disability.[39,40] Therefore, the more significant neurologic problems experienced by males with TSC are likely not only explained by macrostructural disruptions, such as tubers but also by microstructural disruptions in white matter pathways. It has been hypothesized that gender-specific manifestations of TSC may be related to the effects of modifier genes on the X-chromosome and/or the influence of sex hormones, and future studies should seek to clarify this mechanism.

In this study, epilepsy emerged as a significant predictor of the left internal capsule's mean change in ADC, but epilepsy had no effect in either the mean change of ADC or FA properties of any of the white matter tracts. We expected that a history of epilepsy would be correlated with microstructural abnormalities in TSC subjects as early seizure onset is the only clinical risk factor known to be associated with poorer cognitive outcomes in children with TSC,[44–47] and it was a surprise that this was only significant in the left internal capsule (Table 3). There have been several interesting but inconclusive studies documenting differences between the right and left hemispheres in subjects with TSC, with reports of poorer cognition associated independently with both left[10] and right[45,48] hemisphere tuber burden. To our knowledge, left hemisphere MRI findings have not been previously associated with epilepsy in this population. As our study did not control for intelligence and early onset epilepsy has been correlated with lower cognition in TSC, epilepsy may be serving as a proxy for IQ in our group. Alternatively, as seizures are known to affect myelination and tissue microstructure,[49] epilepsy itself or one of the treatments used for it may have a modifying effect on diffusion parameters in subjects with TSC. If so, the left-sided findings described above may be explained by either more frequent left-sided seizures

or by an increased susceptibility of the left hemisphere to the injury caused by seizures. Clearly, a larger study with detailed phenotyping of epilepsy in each subject would be required to answer such questions.

Unlike epilepsy, ASD was not a significant predictor of mean change ADC or FA in any of the white matter tracts investigated. Recent studies report a significant difference in the absolute diffusion parameters for subjects with TSC with and without comorbid ASD in the corpus callosum[18] and arcuate fasciculus.[21] Our results suggest that while the absolute measures may significantly differ, the magnitude of change in FA and ADC over time is not significantly different between TSC subjects with and without ASD. Given that the absolute values of these diffusion parameters are affected but their trajectory of change is not, we hypothesize that white matter in TSC subjects with ASD may suffer from a more static, early insult but thereafter continue to develop along a more normal trajectory. National cohorts investigating imaging findings in newborns and infants with TSC will help test this hypothesis (ClinicalTrials.gov NCT01780441).

A limitation of the study is the short interval (approximately 1 year) between MRI scans for these TSC subjects. As the Boston Children's Hospital Multidisciplinary TSC program expands its enrollment and follows subjects via MRI scans for extended periods of time, the number of subjects will increase and additional time points can be added to track evolving changes in diffusion parameters.

CONCLUSION

This study adds to the literature as it uses HARDI tractography to characterize diffusion properties in the corpus callosum, internal capsule and cingulum bundles in subjects with TSC. Moreover, this study is the first to look at TSC subjects longitudinally over time to gain insight about the developmental trajectory of complete white matter tracts. The development of white matter microstructural diffusivity parameters was more affected in males than in females in the left internal capsule, right and left cingulum bundles, and corpus callosum. Additionally, diffusion parameters were more affected in TSC subjects with epilepsy in the left internal capsule than in subjects without epilepsy. This information will help with the interpretation of imaging changes seen in subjects enrolled in therapeutic trials with mTOR inhibitors.

ACKNOWLEDGEMENTS

This work was supported by Boston Children's Hospital (BCH) and shared instrumentation grants (S10RR023401, S10RR019307, and S10RR023043). MS was supported by NIH U01NS082320, U54 NS092090-01, P30HD018655 and BCH Translational Research Program, and ET was supported by NIH R01HD078561 and R21HD069001. Keh-Li Sheng provided technical assistance.

REFERENCES

1. Ehninger D, Silva AJ. Rapamycin for treating Tuberous sclerosis and Autism spectrum disorders. Trends Mol Med. 2011; 17(2):78–87. [PubMed: 21115397]
2. Han JM, Sahin M. TSC1/TSC2 signaling in the CNS. FEBS Lett. 2011; 585(7):973–980. [PubMed: 21329690]

3. Joinson C, O'Callaghan FJ, Osborne JP, Martyn C, Harris T, Bolton PF. Learning disability and epilepsy in an epidemiological sample of individuals with tuberous sclerosis complex. Psychol Med. 2003; 33(2):335–344. [PubMed: 12622312]
4. Curatolo P, Cusmai R, Cortesi F, Chiron C, Jambaque I, Dulac O. Neuropsychiatric aspects of tuberous sclerosis. Ann N Y Acad Sci. 1991; 615:8–16. [PubMed: 2039170]
5. Winterkorn EB, Pulsifer MB, Thiele EA. Cognitive prognosis of patients with tuberous sclerosis complex. Neurology. 2007; 68(1):62–64. [PubMed: 17200495]
6. de Vries PJ, Hunt A, Bolton PF. The psychopathologies of children and adolescents with tuberous sclerosis complex (TSC): a postal survey of UK families. Eur Child Adolesc Psychiatry. 2007; 16(1):16–24. [PubMed: 17268883]
7. Wong V. Study of the relationship between tuberous sclerosis complex and autistic disorder. J Child Neurol. 2006; 21(3):199–204. [PubMed: 16901420]
8. Curatolo P, Porfirio MC, Manzi B, Seri S. Autism in tuberous sclerosis. Eur J Paediatr Neurol. 2004; 8(6):327–332. [PubMed: 15542389]
9. Jansen FE, van Huffelen AC, Algra A, van Nieuwenhuizen O. Epilepsy surgery in tuberous sclerosis: a systematic review. Epilepsia. 2007; 48(8):1477–1484. [PubMed: 17484753]
10. Jansen FE, Vincken KL, Algra A, et al. Cognitive impairment in tuberous sclerosis complex is a multifactorial condition. Neurology. 2008; 70(12):916–923. [PubMed: 18032744]
11. Mori S, Zhang J. Principles of diffusion tensor imaging and its applications to basic neuroscience research. Neuron. 2006; 51(5):527–539. [PubMed: 16950152]
12. Karadag D, Mentzel HJ, Güllmar D, et al. Diffusion tensor imaging in children and adolescents with tuberous sclerosis. Pediatr Radiol. 2005; 35(10):980–983. [PubMed: 16170442]
13. Firat AK, Karakaş HM, Erdem G, Yakinci C, Biçak U. Diffusion weighted MR findings of brain involvement in tuberous sclerosis. Diagn Interv Radiol. 2006; 12(2):57–60. [PubMed: 16752348]
14. Garaci FG, Floris R, Bozzao A, et al. Increased brain apparent diffusion coefficient in tuberous sclerosis. Radiology. 2004; 232(2):461–465. [PubMed: 15215545]
15. Makki MI, Chugani DC, Janisse J, Chugani HT. Characteristics of abnormal diffusivity in normal-appearing white matter investigated with diffusion tensor MR imaging in tuberous sclerosis complex. AJNR Am J Neuroradiol. 2007; 28(9):1662–1667. [PubMed: 17893226]
16. Simao G, Raybaud C, Chuang S, Go C, Snead OC, Widjaja E. Diffusion tensor imaging of commissural and projection white matter in tuberous sclerosis complex and correlation with tuber load. AJNR Am J Neuroradiol. 2010; 31(7):1273–1277. [PubMed: 20203114]
17. Peng SS, Lee WT, Wang YH, Huang KM. Cerebral diffusion tensor images in children with tuberous sclerosis: a preliminary report. Pediatr Radiol. 2004; 34(5):387–392. [PubMed: 15029464]
18. Peters JM, Sahin M, Vogel-Farley VK, et al. Loss of white matter microstructural integrity is associated with adverse neurological outcome in tuberous sclerosis complex. Acad Radiol. 2012; 19(1):17–25. [PubMed: 22142677]
19. van Eeghen AM, Ortiz-Terán L, Terán LO, et al. The neuroanatomical phenotype of tuberous sclerosis complex: focus on radial migration lines. Neuroradiology. 2013; 55(8):1007–1014. [PubMed: 23644537]
20. Arulrajah S, Ertan G, Jordan L, et al. Magnetic resonance imaging and diffusion-weighted imaging of normal-appearing white matter in children and young adults with tuberous sclerosis complex. Neuroradiology. 2009; 51(11):781–786. [PubMed: 19603155]
21. Lewis WW, Sahin M, Scherrer B, et al. Impaired language pathways in tuberous sclerosis complex patients with autism spectrum disorders. Cereb Cortex. 2013; 23(7):1526–1532. [PubMed: 22661408]
22. Widjaja E, Simao G, Mahmoodabadi SZ, et al. Diffusion tensor imaging identifies changes in normal-appearing white matter within the epileptogenic zone in tuberous sclerosis complex. Epilepsy Res. 2010; 89(2–3):246–253. [PubMed: 20129760]
23. Amarreh I, Dabbs K, Jackson DC, et al. Cerebral white matter integrity in children with active versus remitted epilepsy 5 years after diagnosis. Epilepsy Res. 2013; 107(3):263–271. [PubMed: 24148888]

24. Widjaja E, Kis A, Go C, Raybaud C, Snead OC, Smith ML. Abnormal white matter on diffusion tensor imaging in children with new-onset seizures. Epilepsy Res. 2013; 104(1–2):105–111. [PubMed: 23182414]
25. Shukla DK, Keehn B, Lincoln AJ, Müller RA. White matter compromise of callosal and subcortical fiber tracts in children with autism spectrum disorder: a diffusion tensor imaging study. J Am Acad Child Adolesc Psychiatry. 2010; 49(12):1269–1278. 1278.e1261–1278.e1262. [PubMed: 21093776]
26. Billeci L, Calderoni S, Tosetti M, Catani M, Muratori F. White matter connectivity in children with autism spectrum disorders: a tract-based spatial statistics study. BMC Neurol. 2012; 12:148. [PubMed: 23194030]
27. Ikuta T, Shafritz KM, Bregman J, et al. Abnormal cingulum bundle development in autism: a probabilistic tractography study. Psychiatry Res. 2014; 221(1):63–68. [PubMed: 24231056]
28. Roach ES, Gomez MR, Northrup H. Tuberous sclerosis complex consensus conference: revised clinical diagnostic criteria. J Child Neurol. 1998; 13(12):624–628. [PubMed: 9881533]
29. Northrup H, Krueger DA. Group ITSCC. Tuberous sclerosis complex diagnostic criteria update: recommendations of the 2012 Iinternational Tuberous Sclerosis Complex Consensus Conference. Pediatr Neurol. 2013; 49(4):243–254. [PubMed: 24053982]
30. Tuch DS, Reese TG, Wiegell MR, Wedeen VJ. Diffusion MRI of complex neural architecture. Neuron. 2003; 40(5):885–895. [PubMed: 14659088]
31. D'Arceuil H, Liu C, Levitt P, Thompson B, Kosofsky B, de Crespigny A. Three-dimensional high-resolution diffusion tensor imaging and tractography of the developing rabbit brain. Dev Neurosci. 2008; 30(4):262–275. [PubMed: 17962716]
32. Takahashi E, Dai G, Rosen GD, et al. Developing neocortex organization and connectivity in cats revealed by direct correlation of diffusion tractography and histology. Cereb Cortex. 2011; 21(1): 200–211. [PubMed: 20494968]
33. Takahashi E, Folkerth RD, Galaburda AM, Grant PE. Emerging cerebral connectivity in the human fetal brain: an MR tractography study. Cereb Cortex. 2012; 22(2):455–464. [PubMed: 21670100]
34. Dennis EL, Jahanshad N, McMahon KL, et al. Development of insula connectivity between ages 12 and 30 revealed by high angular resolution diffusion imaging. Hum Brain Mapp. 2014; 35(4): 1790–1800. [PubMed: 23836455]
35. Dennis EL, Jahanshad N, McMahon KL, et al. Development of brain structural connectivity between ages 12 and 30: a 4-Tesla diffusion imaging study in 439 adolescents and adults. Neuroimage. 2013; 64:671–684. [PubMed: 22982357]
36. Takahashi E, Song JW, Folkerth RD, Grant PE, Schmahmann JD. Detection of postmortem human cerebellar cortex and white matter pathways using high angular resolution diffusion tractography: a feasibility study. Neuroimage. 2013; 68:105–111. [PubMed: 23238434]
37. Catani M, Thiebaut de Schotten M. A diffusion tensor imaging tractography atlas for virtual in vivo dissections. Cortex. 2008; 44(8):1105–1132. [PubMed: 18619589]
38. Tillema JM, Leach JL, Krueger DA, Franz DN. Everolimus alters white matter diffusion in tuberous sclerosis complex. Neurology. 2012; 78(8):526–531. [PubMed: 22262746]
39. Sancak O, Nellist M, Goedbloed M, et al. Mutational analysis of the TSC1 and TSC2 genes in a diagnostic setting: genotype--phenotype correlations and comparison of diagnostic DNA techniques in Tuberous Sclerosis Complex. Eur J Hum Genet. 2005; 13(6):731–741. [PubMed: 15798777]
40. Au KS, Williams AT, Roach ES, et al. Genotype/phenotype correlation in 325 individuals referred for a diagnosis of tuberous sclerosis complex in the United States. Genet Med. 2007; 9(2):88–100. [PubMed: 17304050]
41. Bava S, Boucquey V, Goldenberg D, et al. Sex differences in adolescent white matter architecture. Brain Res. 2011; 1375:41–48. [PubMed: 21172320]
42. Giorgio A, Watkins KE, Chadwick M, et al. Longitudinal changes in grey and white matter during adolescence. Neuroimage. 2010; 49(1):94–103. [PubMed: 19679191]
43. Lebel C, Beaulieu C. Longitudinal development of human brain wiring continues from childhood into adulthood. J Neurosci. 2011; 31(30):10937–10947. [PubMed: 21795544]

44. Numis AL, Major P, Montenegro MA, Muzykewicz DA, Pulsifer MB, Thiele EA. Identification of risk factors for autism spectrum disorders in tuberous sclerosis complex. Neurology. 2011; 76(11): 981–987. [PubMed: 21403110]

45. Kaczorowska M, Jurkiewicz E, Domańska-Pakieła D, et al. Cerebral tuber count and its impact on mental outcome of patients with tuberous sclerosis complex. Epilepsia. 2011; 52(1):22–27. [PubMed: 21204819]

46. Vignoli A, La Briola F, Turner K, et al. Epilepsy in TSC: certain etiology does not mean certain prognosis. Epilepsia. 2013; 54(12):2134–2142. [PubMed: 24304436]

47. Zaroff CM, Barr WB, Carlson C, et al. Mental retardation and relation to seizure and tuber burden in tuberous sclerosis complex. Seizure. 2006; 15(7):558–562. [PubMed: 16935530]

48. Kassiri J, Snyder TJ, Bhargava R, Wheatley BM, Sinclair DB. Cortical tubers, cognition, and epilepsy in tuberous sclerosis. Pediatr Neurol. 2011; 44(5):328–332. [PubMed: 21481739]

49. Dwyer BE, Wasterlain CG. Electroconvulsive seizures in the immature rat adversely affect myelin accumulation. Exp Neurol. 1982; 78(3):616–628. [PubMed: 7173373]

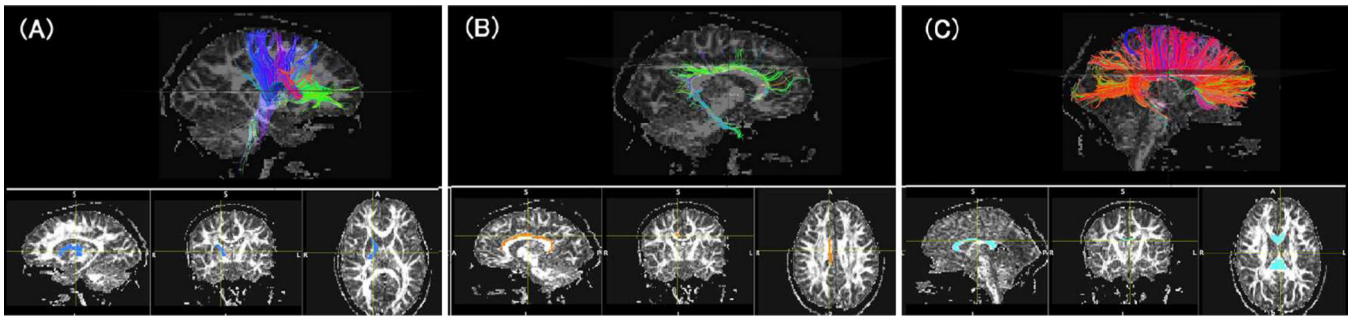

Figure 1.

Examples of tractography pathway identification. The left and right internal capsules (A), the left and right cingulum bundles (B), and the corpus callosum (C) were identified using atlas-based region of interest (ROI) approach (examples of ROIs are shown in the lower row). The color-coding of tractography pathways is based on a standard red-green-blue (RGB) code applied to the vector between the end-points of each fiber (red: left-right, green: anterior-posterior, blue: dorsal-ventral).

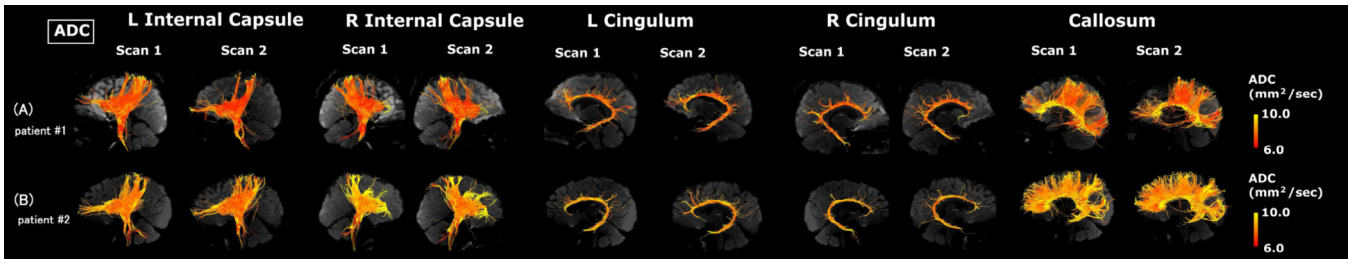

Figure 2.

Examples of tractography pathways from a patient having lower ADC at scan 1 (A) and a patient having higher ADC at scan 1 (B). The color-coding of tractography pathway indicates the magnitude of ADC, as shown by the scale bar on the right.

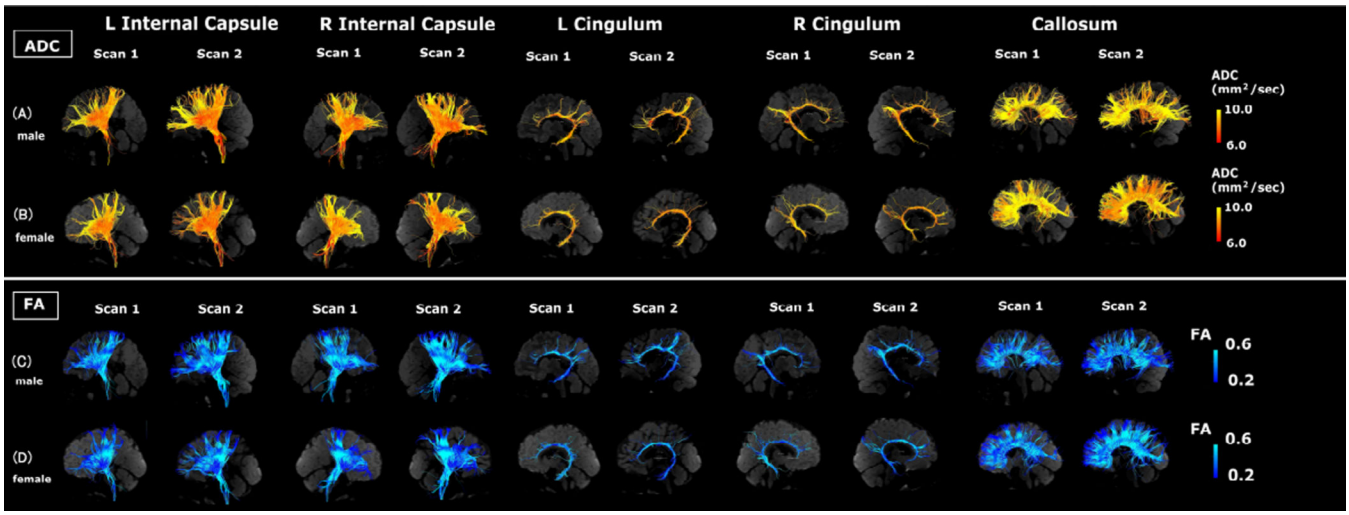

Figure 3.

Examples of tractography pathways showing ADC measures in a male subject (A and C) and a female subject (B and D) at similar ages (male: 2.5 years old [yo] at scan 1 and 3.6 yo at scan 2; female: 2.0 yo at scan 1 and 3.0 yo at scan 2). Please note this figure shows representative images from subjects. The color-coding of tractography pathway indicates the magnitude of ADC, as shown by the scale bar on the right.

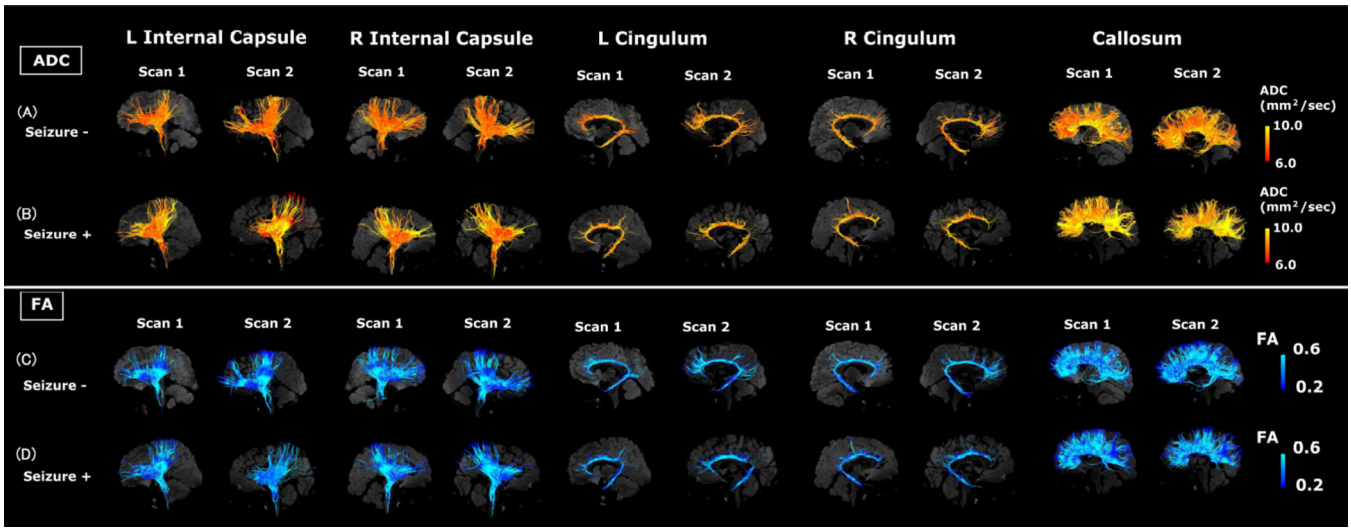

Figure 4.

Examples of tractography pathways showing the ADC values in a subject without epilepsy (A and C) and a patient with epilepsy (B and D) at similar ages (without epilepsy: 4.9 years old [yo] at scan 1 and 5.9 yo at scan 2; with epilepsy: 4.5 yo at scan 1 and 5.3 yo at scan 2). This figure shows representative images from subjects. The color-coding of tractography pathway indicates the magnitude of ADC, as shown by the scale bar on the right.

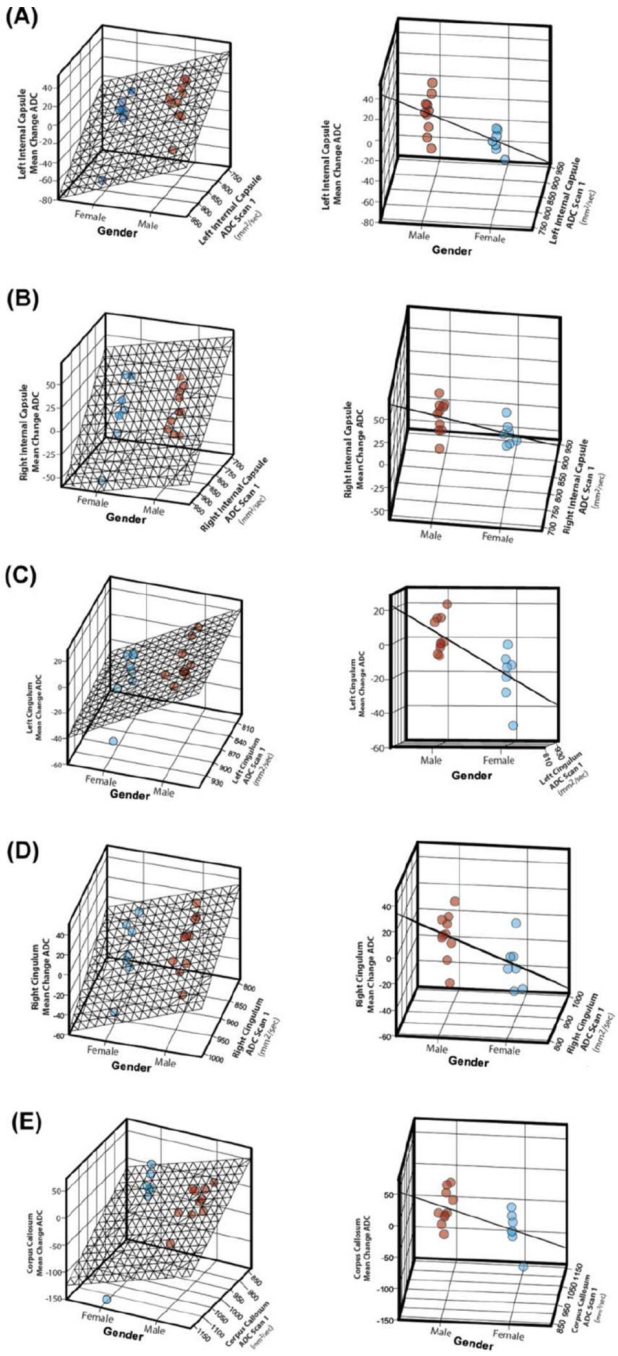

Figure 5.

Relationships among gender, baseline ADC scan measure, and mean ADC changes are illustrated for the left and right internal capsule tracts (A and B), the left and right cingulum bundles (C and D), and the corpus callosum (E). The left and right columns show the same 3-dimensional graphs but at different angles to illustrate the distribution (left column) and standard error (right column) of the mean ADC change data by gender. Blue dots indicate females, and red dots indicate males.

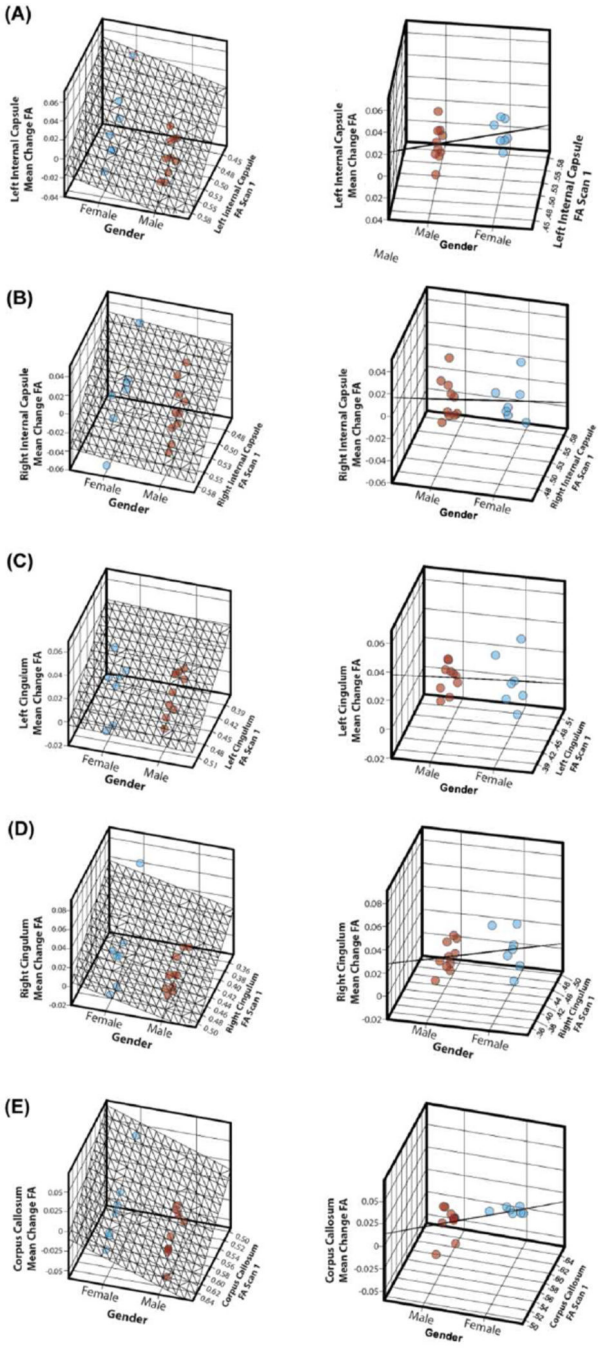

Figure 6.

Relationships among gender, baseline FA scan measure, and mean FA changes are illustrated for the left and right internal capsule (A and B), the left and right cingulum bundles (C and D), and the corpus callosum (E). The left and right columns show the same 3-dimensional graphs but at different angles to illustrate the distribution (left column) and standard error (right column) of the mean ADC change data by gender. Blue dots indicate females, and red dots indicate males.

Table 1

Comparison of Mean Change in ADC and FA from scan 1 to scan 2

		Δ ADC (mm^2/sec)			Δ FA		
		Mean	**Standard Error**	***P***	**Mean**	**Standard Error**	***P***
Right Internal Capsule							
Gender				0.30			0.57
	Male	8.51	6.07		−0.02	0.007	
	Female	−3.72	10.7		−0.01	0.01	
Epilepsy				0.51			0.75
	No	8.10	6.74		−0.02	0.010	
	Yes	0.24	8.54		−0.01	0.007	
ASD				0.24			0.24
	No	7.88	5.81		−0.01	0.006	
	Yes	−7.11	13.2		0.01	0.013	
Left Internal Capsule							
Gender				0.03†			0.40
	Male	3.78	6.17		−0.01	0.005	
	Female	−20.2	7.92		0.01	0.009	
Epilepsy				0.15			0.61
	No	−15.8	4.67		−0.02	0.006	
	Yes	0.76	8.42		−0.01	0.008	
ASD				0.89			0.27
	No	−6.75	5.33		−0.02	0.005	
	Yes	−4.45	15.2		−0.003	0.012	
Right Cingulum							
Gender				0.07			0.17
	Male	2.40	5.95		0.003	0.003	
	Female	−17.0	8.12		0.02	0.010	
Epilepsy				0.70			0.89

		Δ ADC (mm^2/sec)			Δ FA		
		Mean	**Standard Error**	***P***	**Mean**	**Standard Error**	***P***
	No	−8.15	6.96		0.01	0.005	
	Yes	−3.78	7.74		0.01	0.007	
ASD				0.94			0.18
	No	−5.86	5.93		0.004	0.004	
	Yes	−4.91	12.0		0.02	0.012	
Left Cingulum							
Gender				0.002†			0.83
	Male	3.65	3.21		0.01	0.003	
	Female	−19.8	6.00		0.02	0.009	
Epilepsy				0.35			0.93
	No	−10.8	3.79		0.01	0.006	
	Yes	−2.61	6.51		0.01	0.006	
ASD				0.98			0.25
	No	−6.08	8.94		0.01	0.004	
	Yes	−5.8	17.9		0.02	0.01	
Corpus Callosum							
Gender				0.21			0.04†
	Male	−4.60	6.40		−0.02	0.006	
	Female	−29.2	20.71		0.003	0.009	
Epilepsy				0.67			0.67
	No	−9.73	7.29		−0.01	0.016	
	Yes	−18.3	15.5		−0.01	0.028	
ASD				0.36			0.20
	No	−5.88	5.61		−0.02	0.006	
	Yes	−36	29.0		0.001	0.013	

Abbreviations: FA, fractional anisotropy; ADC (mm^2/sec), apparent diffusion coefficient

† $p \leq 0.05$.

Table 2

Correlation analyses with Age

	Age 1‡ (Time point 1)		Age 2‡ (Time point 2)	
	Pearson's r	***P***	**Pearson's r**	***p***
Left Internal Capsule				
ADC Scan 1	−0.56†	0.02†	−0.59†	0.01†
FA Scan 1	0.47	0.06	0.59†	0.01†
Change in ADC	0.10	0.70	0.11	0.69
Change in FA	−0.03	0.90	−0.14	0.59
Right Internal Capsule				
ADC Scan 1	−0.62†	0.007†	−0.52†	0.03†
FA Scan 1	0.48	0.05	0.52†	0.03†
Change in ADC	0.46	0.06	0.49	0.05†
Change in FA	−0.12	0.67	−0.18	0.50
Left Cingulum				
ADC Scan 1	−0.51†	0.04†	−0.55†	0.02†
FA Scan 1	0.53†	0.03†	0.57†	0.02†
Change in ADC	0.01	0.96	−0.06	0.82
Change in FA	−0.20	0.44	−0.30	0.27
Right Cingulum				
ADC Scan 1	−0.47	0.06	−0.33	0.20
FA Scan 1	0.45	0.07	0.51	0.04†
Change in ADC	0.42	0.09	0.40	0.11
Change in FA	−0.08	0.77	−0.10	0.70
Corpus Callosum				
ADC Scan 1	−0.34	0.18	−0.88	0.74
FA Scan 1	0.26	0.32	0.28	0.28
Change in ADC	0.45	0.07	0.55	0.02†
Change in FA	−0.13	0.62	−0.19	0.47

Abbreviations: FA, fractional anisotropy; ADC (mm^2/sec), apparent diffusion coefficient

‡Correlation analyses are performed with age and the scan measures at the respective time point (i.e., Age 1 and corresponding scan measure at time point 1; Age 2 and corresponding scan measure at time point 2)

†$p \leq 0.05$.

Table 3

Multiple regression analysis for identifying predictors of Mean Change ADC

Model	Variable	Unstandardized coefficients B	Standard error	*P*
Left Internal Capsule				
1	ADC Scan 1†	−0.43	0.17	0.03†
	Age	−1.36	1.35	0.33
2	ADC Scan 1†	−0.32	0.12	0.02†
	Gender	−23.3	8.29	0.01†
3	ADC Scan 1†	−0.40	0.12	0.006†
	Epilepsy†	22.5	8.74	0.02†
4	ADC Scan 1†	−0.40	0.15	0.02†
	ASD	13.3	11.5	0.27
Right Internal Capsule				
1	ADC Scan 1†	−0.36	0.13	0.02†
	Age	0.21	1.27	0.87
2	ADC Scan 1†	−0.37	0.94	0.001‡
	Gender	13.1	8.14	0.13
3	ADC Scan 1†	−0.40	0.11	0.003†
	Epilepsy	6.23	9.56	0.53
4	ADC Scan 1†	−0.37	0.12	0.006†
	ASD	0.55	10.69	0.96
Left Cingulum				
1	ADC Scan 1	−0.03	0.16	0.88
	Age	−0.05	1.17	0.97
2	ADC Scan 1	−0.06	0.10	0.56
	Gender†	−23.8	6.44	0.002†
3	ADC Scan 1	−0.09	0.15	0.54
	Epilepsy	10.7	9.51	0.28
4	ADC Scan 1	−0.20	0.14	0.87
	ASD	0.59	9.91	0.95
Right Cingulum				
1	ADC Scan 1	−0.13	0.13	0.36
	Age	1.45	1.27	0.27
2	ADC Scan 1	−0.21	0.11	0.07
	Gender	−20.1	9.02	0.04
3	ADC Scan 1	−0.23	0.13	0.08
	Epilepsy	10.2	10.6	0.35
4	ADC Scan 1	−0.22	0.127	0.11

Model	Variable	Unstandardized coefficients B	Standard error	*P*
	ASD	6.34	11.64	0.60
Corpus Callosum				
1	ADC Scan 1†	−0.24	0.111	0.05†
	Age	2.42	1.88	0.22
2	ADC Scan 1†	−0.32	0.096	0.005†
	Gender	−31.8	14.64	0.05†
3	ADC Scan 1†	−0.32	0.12	0.02†
	Epilepsy	12.0	18.13	0.52
4	ADC Scan 1	−0.26	0.125	0.05†
	ASD	−9.32	20.48	0.66

Abbreviations: ASD, autism spectrum disorder; ADC (mm^2/sec), apparent diffusion coefficient ; Age (years)

Reference: Gender, 0= male; Epilepsy, 0= no epilepsy; ASD, 0=no ASD

† $p \leq 0.05$;

‡ $p \leq 0.001$.

Table 4

Multiple regression analysis for identifying predictors of Mean Change FA

Model	Variable	Unstandardized coefficients B	Standard error	*P*
Left Internal Capsule				
1	FA Scan 1†	−0.59	0.16	0.002†
	Age	0.002	0.001	0.12
2	FA Scan 1†	−0.44	0.14	0.006†
	Gender	0.014	0.008	0.09
3	FA Scan 1†	−0.52	0.14	0.003†
	Epilepsy	−0.01	0.008	0.15
4	FA Scan 1†	−0.45	0.16	0.01†
	ASD	0.005	0.009	0.62
Right Internal Capsule				
1	FA Scan 1†	−0.59	0.18	0.005†
	Age	0.001	0.001	0.30
2	FA Scan 1†	−0.50	0.16	0.009†
	Gender	0.006	0.009	0.54
3	FA Scan 1†	−0.51	0.17	0.009†
	Epilepsy	−0.003	0.010	0.74
4	FA Scan 1†	−0.47	0.01	0.014†
	ASD	0.007	0.17	0.49
Left Cingulum				
1	FA Scan 1†	−0.313	0.11	0.02
	Age	0.001	0.001	0.52
2	FA Scan 1†	−0.27	0.10	0.01
	Gender	−0.002	0.007	0.77
3	FA Scan 1†	−0.33	0.100	0.005
	Epilepsy	−0.010	0.007	0.18
4	FA Scan 1†	−0.26	0.101	0.02
	ASD	0.005	0.008	0.53
Right Cingulum				
1	FA Scan 1†	−0.37	0.13	0.01†
	Age	0.001	0.001	0.34
2	FA Scan 1†	−0.31	0.11	0.01†
	Gender	0.013	0.008	0.12
3	FA Scan 1†	−0.41	0.12	0.004†
	Epilepsy	−0.02	0.008	0.11

Model	Variable	Unstandardized coefficients B	Standard error	*P*
4	FA Scan 1†	−0.29	0.13	0.04†
	ASD	0.005	0.01	0.61
Corpus Callosum				
1	FA Scan 1†	−0.46	−0.67	0.007†
	Age	0.0002	0.04	0.84
2	FA Scan 1‡	−0.46	0.10	0.0004‡
	Gender	0.02	0.007	0.003†
3	FA Scan 1†	−0.50	0.13	0.002†
	Epilepsy	−0.01	0.009	0.14
4	FA Scan 1†	−0.43	0.15	0.01†
	ASD	0.004	0.01	0.73

Abbreviations: ASD, autism spectrum disorder; FA, fractional anisotropy; Age (years)

Reference: Gender, 0= male; Epilepsy, 0= no epilepsy; ASD, 0=no ASD

† $p \leq 0.05$;

‡ $p \leq 0.001$.